Model of the IHC-AN synapse: Power-law adaptation in the discharge rates of auditory-nerve fibers

Muhammad S. A. Zilany [1,2], Ian C. Bruce [2], Paul C. Nelson [3], Laurel H. Carney [1]

[1] University of Rochester, Rochester, NY, USA; [2] McMaster University, Hamilton, ON, Canada; [3] Johns Hopkins University, Baltimore, MD, USA

INTRODUCTION

At the first synapse of the auditory pathway, the receptor potential of the inner hair cell (IHC) is converted into a firing pattern in the auditory-nerve (AN) fibers, where adaptation in discharge rate is observed. The IHC-AN synapse complex is believed to be mainly responsible for this adaptation. Several computational models have been developed to describe how depletion of synaptic vesicles in the synapse could give rise to exponential adaptation. However, these models are unable to accurately predict several sets of AN data, including amplitude-modulation transfer functions, long-term adaptation, forward masking, and adaptation to increments and decrements in the amplitude of an ongoing stimulus.

There is growing evidence that dynamics of biological systems that appear exponential over short term are in some cases better described by power-law dynamics. In this work, we describe a model of rate adaptation at the IHC-AN synapse that utilizes both exponential and power-law dynamics rather than only exponential adaptation. The resulting model is capable of addressing all of the responses mentioned above.

DESCRIPTION OF THE MODEL

A. Model of the Auditory-periphery

❖ The auditory-periphery model (Zilany and Bruce, 2006) has most of the **nonlinearities** seen in the AN responses (e.g., **nonlinear tuning**)

❖ Classical models of neurotransmitter vesicle release in the IHC-AN synapse have the same double-exponential adaptation at both onset and offset. However, experimental data has different dynamics in the onset and offset responses. Thus, these models fail to account for responses in the stimulus offset, as well as other long-term response properties in the AN.

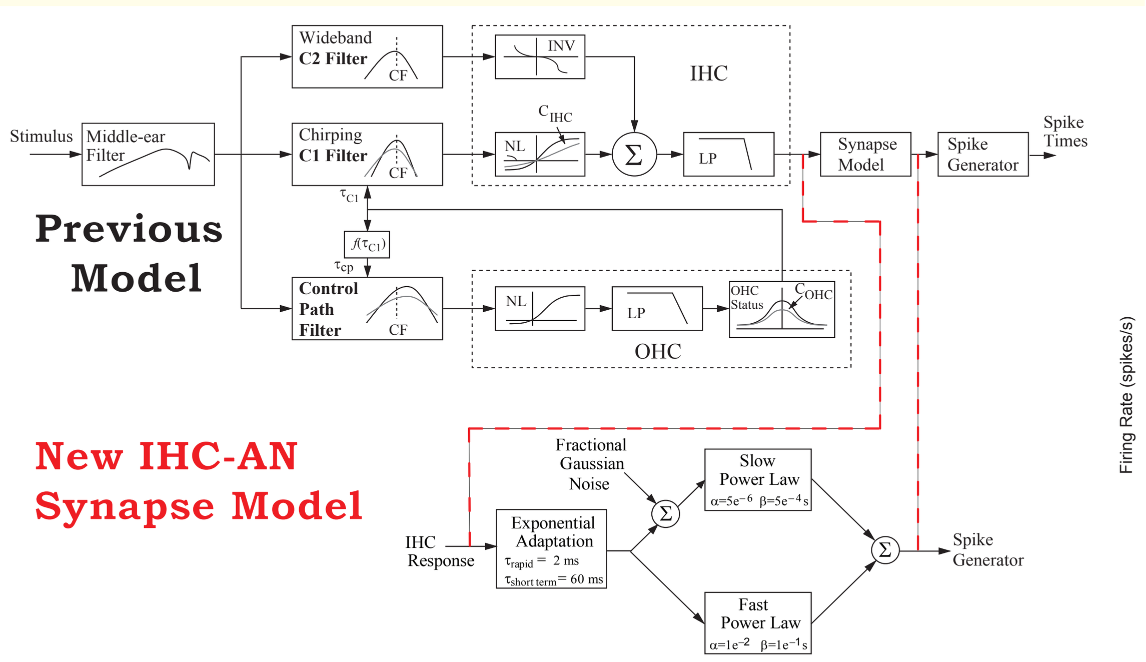

FIG 1. Schematic diagram of the auditory-periphery model. From Zilany and Bruce (2006). **New IHC-AN synapse model**: Exponential adaptation (three store diffusion model, Westerman and Smith, 1988) followed by parallel power law adaptation models (slow and fast). Fractional Gaussian noise added at the input of the slow power law adaptation model results in desired distribution of spontaneous rate in the output.

❖ We hypothesized that power-law adaptation following exponential adaptation can account for responses in the stimulus offset, long-term response properties, as well as adaptation to increments and decrements in the amplitude of an ongoing stimulus.

B. Power-Law Synapse Model

❖ The adapted response, r(t), is linearly related to the input stimulus, S(t).

❖ The suppressive effects, I(t), are accumulated with power-law dynamics (Drew and Abbott, 2006). We have computed this by convolving r(t) with the impulse response of the power-law function.

❖ The much longer **"tail"** on the power-law function produces a longer memory for past responses than does exponential adaptation.

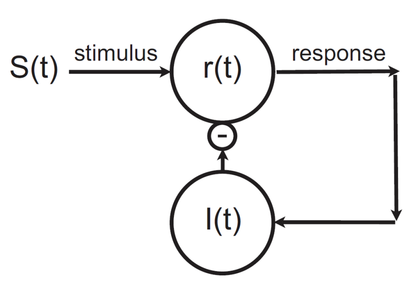

From Drew and Abbott, 2006

$$r(t) = \max\left[0,\ S(t) - I(t)\right]$$

$$I(t) = \alpha \int_0^t dt' \frac{r(t')}{t - t' + \beta}$$

RESULTS

A. Spontaneous Activity

Distributions of Spontaneous Rates

❖ Jackson and Carney (2005) showed that only two or three spont rates with long-term fluctuations were able to describe the distribution of spont rates of the AN fibers. We have modeled this phenomenon by long-range dependent Fractional Gaussian Noise (added in the slow power-law adaptation path) that gives the desired bimodal histogram of the AN spontaneous rates.

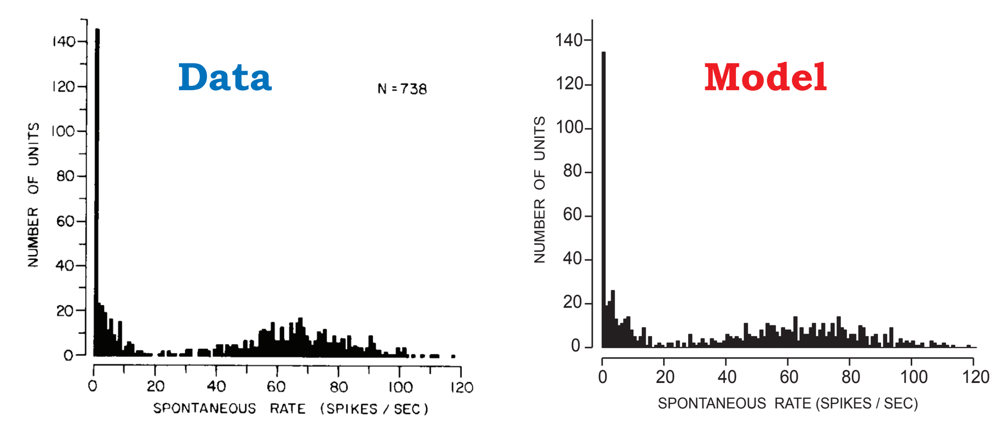

FIG 2. Histogram of **Data** (Liberman, 1978) and **Model** spontaneous-rate (SR) estimates from 30-sec recordings from 738 fibers in the auditory nerves of cats (binwidth 1 spike/sec).

B. Responses to Pure Tones at CF

Recovery of Spontaneous Activity

❖ The offset response is characterized by a pause in the response followed by a slow recovery of spontaneous activity. Fibers with low spontaneous rates exhibit slower recovery than high spontaneous rate fibers.

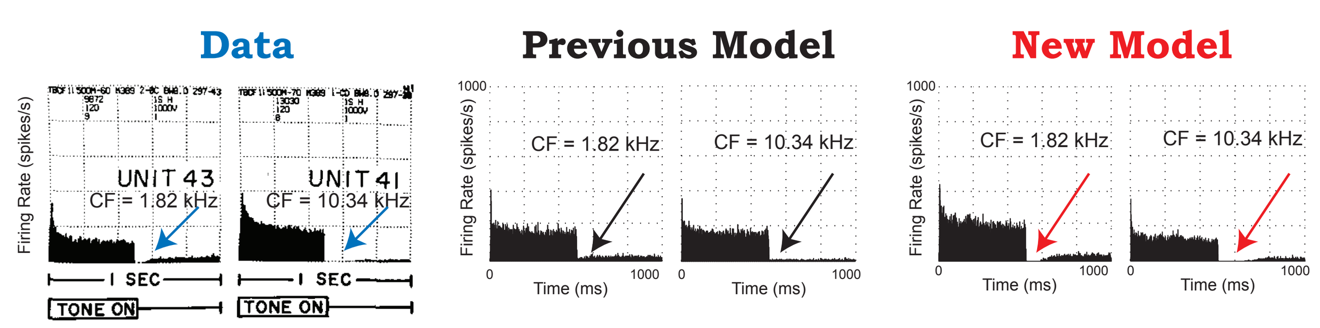

FIG 3. Effects of spontaneous rate on recovery in **Data** and **Model** histograms of two AN fibers in response to 500-ms duration constant-amplitude stimuli. **Data**: From Kiang (1965). **Previous** and **New Model** histograms at 25 dB SPL.

Long-Term Recovery

❖ As the exposure level increases, the time constant of recovery increases, even though the rate-level response saturates at higher levels.

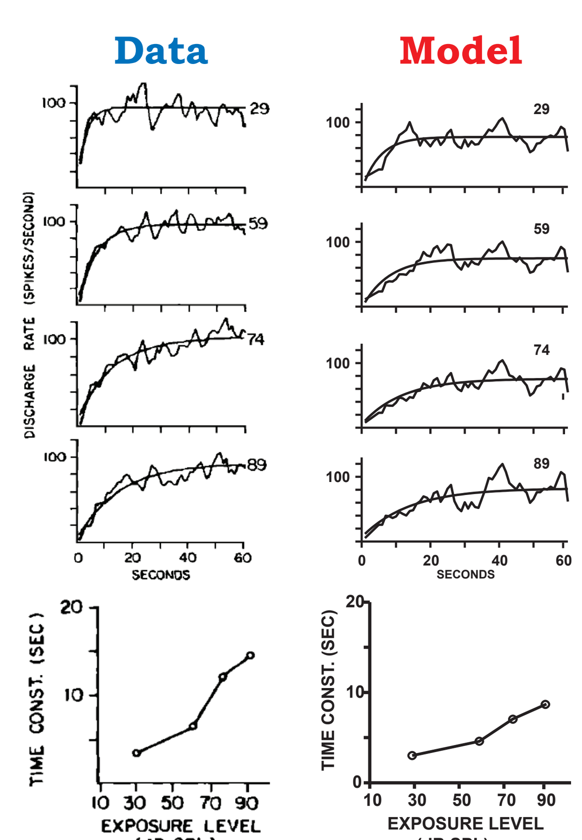

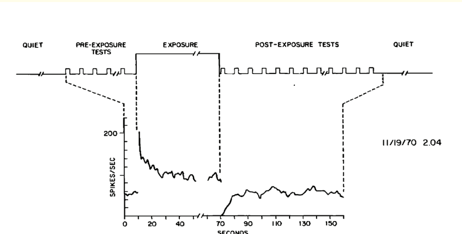

FIG 4. Effect of exposure level on recovery for an AN fiber of CF at 2.15 kHz. Duration of the exposure signal was 60 sec. The test signal (100-ms long applied once per second) was also at CF with level 19 dB SPL (fixed). Total durations of the pre- and post-exposure test signals were 10 and 60 secs, respectively. Recovery of the post-exposure responses (fitted to an exponential) is shown with their corresponding time constant values. **Data**: From Young and Sachs (1973). **Model** responses to 10 repetitions of the same stimulus were averaged.

C. Tones with Change in Amplitude

❖ Responses are additive irrespective of the delay (between onset and increment/decrement) for both small and large windows, except for small window onset responses to the decrement. Inclusion of the fast power-law component in the model helps to achieve this.

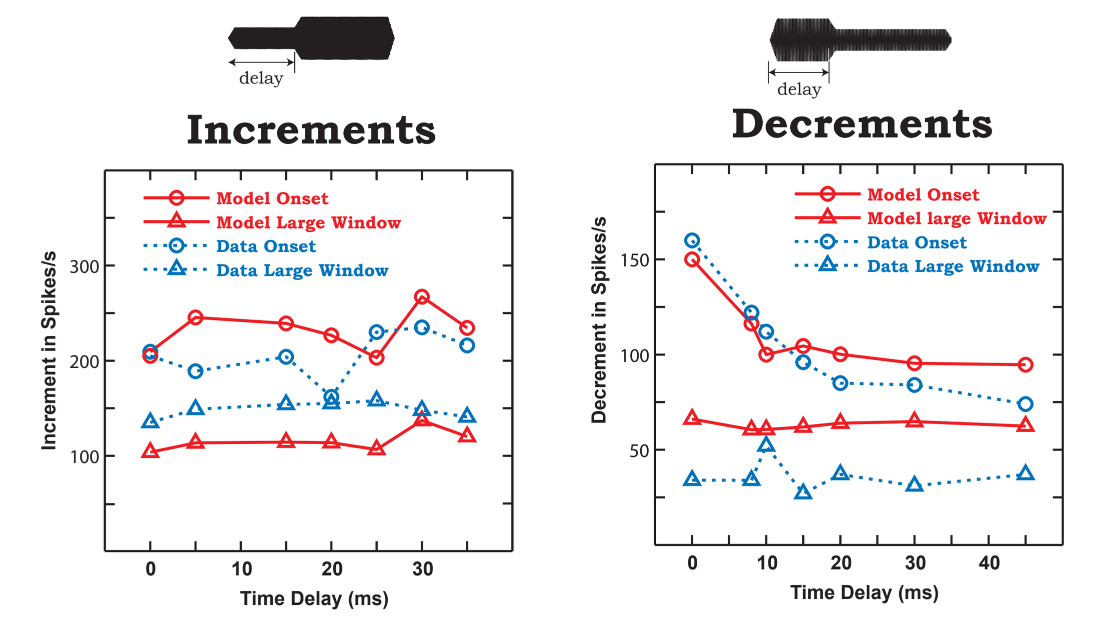

FIG 5. Effects of prior adaptation on increment and decrement responses. The stimulus was a 60-ms CF tone 13 dB above threshold, and subsequently levels were either increased or decreased by 6 dB at different delays from onset. Changes in rate responses for both onset (first 0.64 ms, circles) and large window (first 10.2 ms, down triangles) are shown. **Data** from Smith et. al., 1985; **Model** responses: solid lines with symbols.

D. Forward Masking

Probe Response vs. Delay (Masker and Probe)

❖ Probe responses are increasingly suppressed as the delay between the masker and the probe becomes smaller.

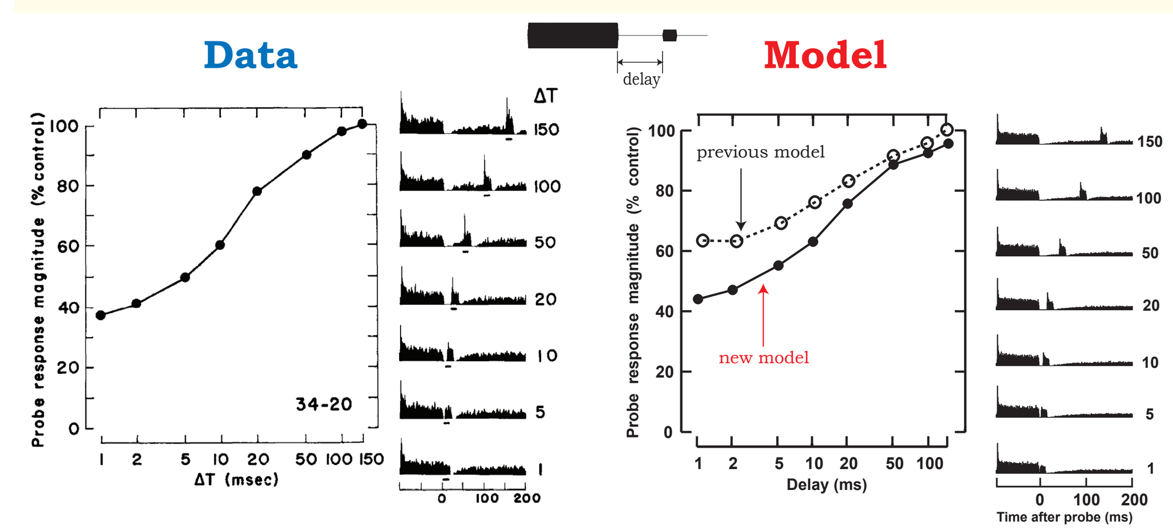

FIG 6. **Data** (Harris and Dallos, 1979) and **Model** poststimulus recovery as a function of delay between masker offset and probe onset. Masker: 2.75 kHz tone (fiber's CF), 30 dB above threshold (+30 dB), 100 ms duration. Probe stimulus: 2.75 kHz tone, +20 dB, 15 ms duration.

Forward Masking Population Responses

❖ As the masker level increases, probe responses are increasingly suppressed as the delay between the masker and the probe becomes smaller.

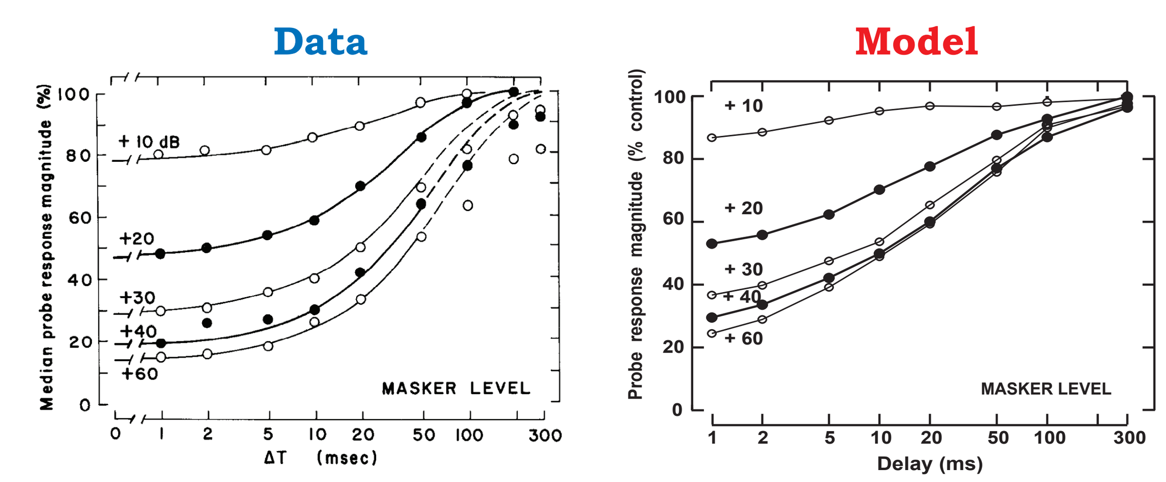

FIG 7. **Data** (Harris and Dallos, 1979) and **Model** forward masking recovery functions for a population of fibers; masker level is the parameter. Masker stimuli were tones with frequency match to CF, 100 ms duration. Probe stimuli were also tones at CF, +20 dB, 15 ms duration.

E. Amplitude-Modulated (AM) Tones

Effect of Depth on Synchrony

❖ As the modulation depth of the sinusoidal AM stimulus increases, the poststimulus time histograms (psths) become more peaky, although modulation gain decreases with increasing modulation depth.

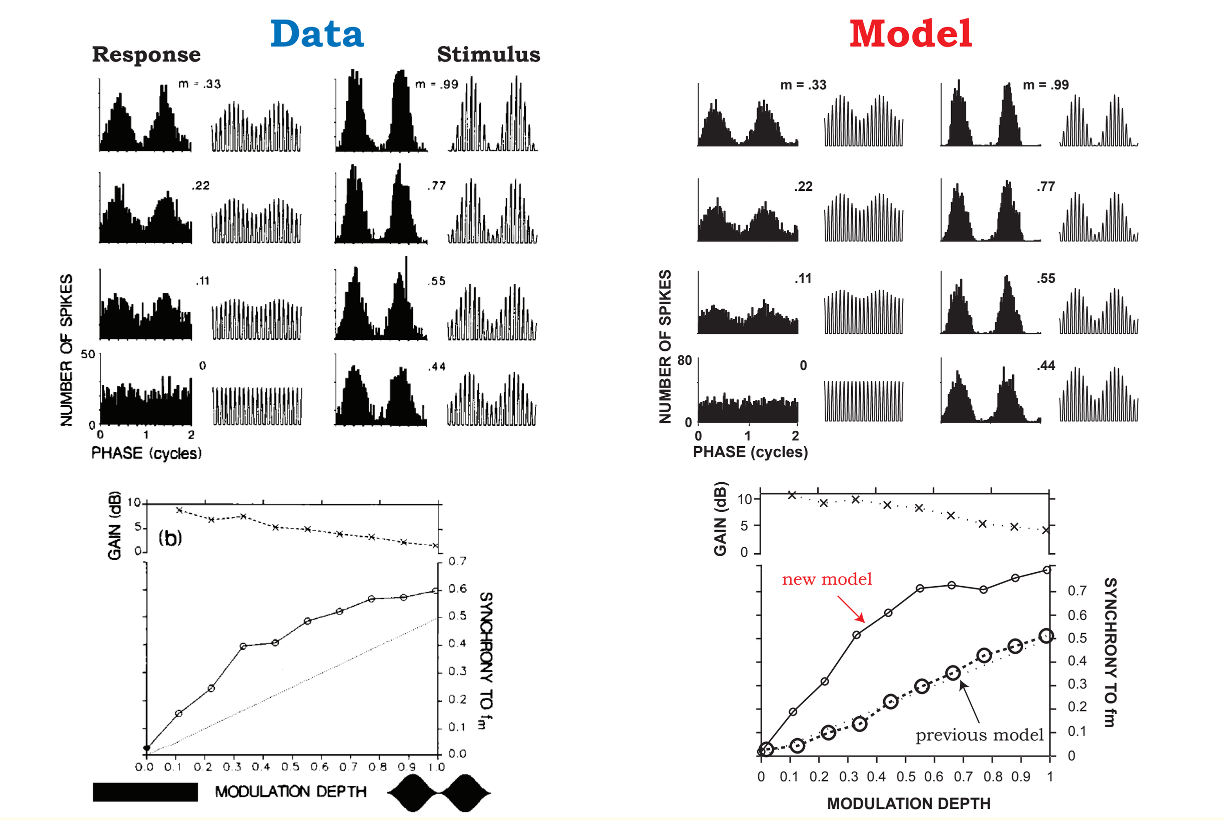

FIG 8. Effect of increasing modulation depth (m) on synchrony for an actual **Data** (Joris and Yin, 1992) and **Model** fiber with CF at 20.2 kHz, high spontaneous rate fiber, in response to amplitude-modulated tones with carrier frequency matched to CF, modulation frequency (fm) = 100 Hz, and level at +10 dB above threshold.

Modulation Transfer Function (MTF)

❖ MTFs are characterized by low-pass filter shapes with cut-off frequency around 1 kHz, sharp roll-off, and positive gain (0-5 dB) in the low-pass region.

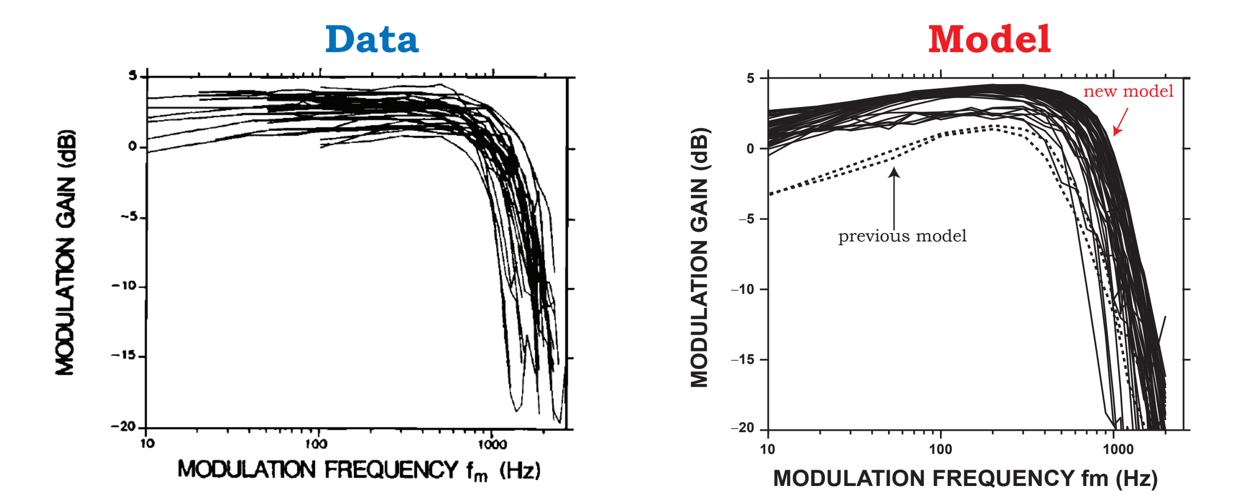

FIG 9. **Data** (Joris and Yin, 1992) and **Model** MTFs of high CF (> 10 kHz) fibers.

DISCUSSION

❖ The new model with power-law dynamics is more successful at describing several AN response properties than previous models having only exponential adaptations.

❖ The slowly adapting component with power-law dynamics significantly improves the AN response at stimulus offset and the recovery behavior.

❖ The fast path with power-law dynamics contributes to the unsaturated onset response, to the additivity observed in AN rate responses to stimuli with amplitude increments, and also to the responses of amplitude-modulated signals (MTFs).

References

[1] Zilany, M. S. A. and Bruce, I. C. (2006). "Modeling auditory-nerve responses for high sound pressure levels in the normal and impaired auditory periphery," J. Acoust. Soc. Am., 120(3), 1446–1466.

[2] P. J. Drew, P. J. and Abbott L. F. (2006). "Models and properties of power-law adaptation in neural system," J. physiol, 96, 826–833.

[3] Westerman, L. A. and Smith, R. L. (1988). "A diffusion model of the transient response of the cochlear inner hair cell," J. Acoust. Soc. Am., 83, 2266–2276.

[4] Liberman, M. C. (1978). "Auditory-nerve response from cats raised in a low-noise chamber," J. Acoust. Soc. Am., 63(2), 442–455.

[5] Jackson, B. J. and Carney, L. H. (2005). "The spontaneous-rate histogram of the auditory nerve can be explained by only two or three spontaneous rates and long-range dependence ," J. Asso. Res. Oto., 6, 148–159.

[6] Kiang, N. Y-S. (1965). "Discharge patterns of single fibers in the cat's auditory nerve," M.I.T. Research Monograph No. 35 (M.I.T. Press, Cambridge, MA).

[7] Young, E. and Sachs, M. B. (1973). "Recovery from sound exposure in auditory-nerve fibers," J. Acoust. Soc. Am., 54(6), 1535–1543.

[8] Smith, R. L., Brachman, M. L., and Frisina, R. D. (1985). "Sensitivity of auditory-nerve fibers to changes in intensity: A dichotomy beween decrements and increments," J. Acoust. Soc. Am., 78(4), 1310–1316.

[9] Harris, D. M. and Dallos, P. (1979). "Forward masking of auditory nerve fiber responses," J. neurophysiol, 42(4), 1083–1107.

[10] Joris, P. X. and Yin, T. C. (1992). "Responses to amplitude-modulated tones in the auditory nerve of the cat," J. Acoust. Soc. Am., 91(1), 215–232.

[This work is supported by NIH-NIDCD R01-01641, F32-009164, and CIHR NET Grant 54023]